Research Journal of Pharmaceutical, Biological and Chemical Sciences

Synthesis and Spectroscopic Analytical Techniques Studies of Zn (II), Pt (IV) and Au (III) lisinopril Drug Complexes.

Abeer A. El-Habeeb*

Department of Chemistry, Faculty of Science, Princess Nora Bint Abdul Rahman University, Riyadh, Kingdom Saudi Arabia.

ABSTRACT

Three lisinopril hypertensive drug complexes of Zn(II), Au(III) and Pt(IV) were prepared and discussed upon different analytical techniques like elemental analysis, conductometry, UV–Vis, IR, ^{1}H-NMR spectroscopy, X-ray powder diffraction, scanning electron microscopy (SEM) and thermal analysis. The infrared spectroscopic data led to the coordinated of LIS ligand as a mono- or di- basic bidentate ligand towards the central metal ion through the oxygen atom of –COOH group after deprotonated. From the microanalytical data, the stoichiometry of the complexes is 1:2 or 1:1 (Metal: ligand) was found. The ligand and their metal complexes were scanned for antimicrobial activity against (*Escherichia coli*, and *Staphylococcus aureus*) and fungicidal activity against (*Aspergillus flavus* and *Candida albicans*).

Keywords: Lisinopril; gold; platinum; infrared; thermal; biological activity.

Corresponding author
Email: drabeerhabeeb@yahoo.com

INTRODUCTION

Many metallic elements play a crucial role in living systems. Metal ions are electron deficient, whereas most biological molecules such as proteins and DNA are electron rich. The attraction of these opposing charges leads to a general tendency for metal ions to bind to and interact with biological molecules [1]. This activity of metal ions has started the development of metal based drugs with promising pharmacological application and may offer unique therapeutic opportunities [2-4]. Concerning the relationship between the metal ions and hypertensive drugs as a main task of this work, the literature survey introduced that the angiotensin-converting enzyme (ACE) inhibitors has an important role as a therapeutic agents in the treatment of hypertension and congestive heart failure [5, 6]. Since ACE is a zinc-metallopeptidase which activated by chloride. The mechanism of action of ACE inhibitors results mainly from competition with the natural substrate by binding to the zinc ion in the active site on the ACE molecule.

Lisinopril (LIS; Fig. 1), chemically known as (1-[6-amino-2-(1-carboxy-3-phenyl-propyl)amino-hexanoyl] pyrrolidine-2- carboxylic acid dehydrate) [7]. It is a drug of the angiotensin converting enzyme (ACE) inhibitor class, due to its safe and effective properties, lisinopril is widely used in the therapy of essential hypertension, congestive heart failure (CHF), heart attacks and also in preventing renal and retinal complication of diabetes [8]. Historically, lisinopril was the third ACE inhibitor, after captopril and enalapril, and was introduced into therapy in the early 1990s. The official analytical methods described for lisinopril are potentiometric titration and HPLC [9-12]. The therapeutic importance of lisinopril was behind the development of numerous methods for its determination. Several analytical methods have been applied for the determination of lisinopril in biological samples and pharmaceutical preparations such as, spectrophotometry [13], high performance liquid chromatography (HPLC) [14], high performance thin-layer chromatography (HPTLC) [15], and capillary electrophoresis (CE) [16], fluoroimmunoassay [17], radioimmuoassay [18], fluorozmatic assay [19].
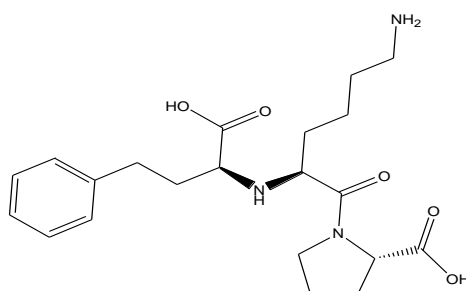
Figure 1: Structure of Lisinopril (LIS) drug.

Lisinopril has two carboxyl groups including prolyl COOH and central COOH, which can interact with metal ions, makes lisinopril a good chelating ligand. In pH 3.5 solution, only central COOH was dissociated to carboxylate ion and own a high electronic density to easily interact with metal ions than the un-dissociated prolyl COOH. Above pH 5.0 solution, both COOH groups were in a dissociation form. Lisinopril was mostly dissociated in pH 7.3 solutions [20]. However, literature survey has revealed that very little attempt has been made to study the complexes of transition metal ions with the above mentioned drug ligand [20-22]. It is a thought of interest to study the synthesis and characterization, thermal behavior, and biological screening of the new transition metal complexes of Zn(II), Au(III) and Pt(IV) with lisinopril drug molecule. The processes of thermal degradation of the ligands and their metal complexes have been investigated by thermoanalytical method (TG/DTG). The Coats-Redfern and Horowitz-Metzeger integral methods have been used to determine the associated kinetic parameters for the successive steps in the decomposition sequence. Drug compounds are biologically active; these compounds have become of interest to be studied biologically, and compared their activities against some species of gram positive and gram negative bacteria as well as two fungal species.

EXPERIMENTAL

Materials

All chemicals pure; lisinopril drug, $AuCl_3$, $PtCl_4$, $ZnCl_2$, and solvents (ethanol and dimethylsulfoxide DMSO) were commercially available from BDH and were used without further purification.

Preparation of complexes

All the prepared complexes under investigation were synthesized similarly according to the following procedure:

In general, 1 mmol of pure lisinopril drug ligand was dissolved in 25 mL of ethanol then mixed with 25 mL of hot ethanolic solution of 2 mmol of metal chlorides (Au(III), Pt(III) and Zn(II)). A mixtures with molar ratio of 2:1 (M: ligand) were adjusted at pH = 8–9 using 1 M ethanolic ammonia solution. The neutralized mixtures were refluxed with continuous stirring at 60–70 ^{o}C for about 4 h. The mixtures were left overnight until precipitated. The precipitates obtained were filtered off and washed several times using methanol then left over anhydrous calcium chloride. The yield percent of the products collected were about 60–70%.

Analyses

Spectral and analytical measurements

IR spectra of the metal complexes were recorded on Bruker infrared spectrophotometer as potassium bromide pellets, and in the range 400–4000 cm^{-1}. The electronic spectra of the complexes were measured in DMSO solvent with concentration of 1×10^{-3} M, in rang 200–1100 nm by using Unicam UV/Vis spectrometer. The proton NMR spectra were recorded on a Varian FT- 300 MHz spectrometer in d_6-DMSO solvent, using TMS as internal standard. SEM images were obtained using a Jeol Jem-1200 EX II Electron Microscope at an acceleration voltageof 25 kV. The samples were coated with a gold plate. X-ray diffraction (XRD) patterns of the samples were recorded on a X Pert Philips X-ray diffractometer. All the diffraction patterns were obtained by using CuKα1 radiation, with a graphite monochromator at 0.02 ^{o}/min scanning rate. Carbon, hydrogen and nitrogen analysis of the complexes have been carried out in Vario EL Fab. CHNS. The amount of water and the metal content percentage were determined by thermal analysis methods. The molar conductance of 10^{-3} M solutions of the lisinopril ligand and their metal complexes in DMSO solvent were measured on a HACH conductivity meter model. All the measurements were taken at room temperature for freshly prepared solutions. Stuart Scientific electro thermal melting point apparatus was used to measure the melting points of the ligand and their metal complexes in glass capillary tubes in degrees Celsius. The effective magnetic moment (μ_{eff}) values of the solid complexes were measured at room temperature using Gouy's method by a magnetic susceptibility balance from Johnson Metthey and Sherwood model. Thermogravimetric Analysis (TGA) experiments were conducted using Shimadzu TGA-50H thermal analyzers. All experiments were performed using a single loose top loading platinum sample pan under nitrogen atmosphere at a flow rate of 30 mL/min and a 10 ^{o} C/min heating rate for the temperature range 25–800 ^{o} C.

Biological screening

The lisinopril drug and their metal complexes were tested against two species of bacteria (*S. aureus* and *E. coli*) and two fungal species (*A. flavus* and *C. albicans*) using modified Kirby-Bauer disc diffusion method [23]. The screened compounds were dissolved individually in DMSO (dimethylsulfoxide) in order to make up a solution of 1000 lg/mL concentration for each of these compounds. Filter paper discs (Whatman No. 1 filter paper, 5 mm diameter) were saturated with the solution of these compounds. The discs were placed on the surface of solidified Nutrient agar dishes seeded by the tested bacteria or Czapek's Dox agar dishes seeded by the tested fungi. The diameters of inhibition zones (mm) were measured at the end of an incubation period, which was 24 h at 37 ^{o} C for bacteria, and 4 days at 28 ^{o} C for fungi. Discs saturated with DMSO are used as solvent control.

RESULTS AND DISCUSSIONS

Physical and molar conductance data

The metal complexes of LIS with Au(III), Pt(IV), and Zn(II) were synthesized. Some physical properties and analytical data of the new three complexes were summarized in Table 1. The satisfactory elemental analysis results (Table 1) show that the metal complexes with lisinopril drug were of 2:1 (metal: LIS) molar ratio except for Pt(IV) was of 1:1 (metal: LIS) molar ratio. The Au(III), Pt(IV), and Zn(II) synthesized complexes have light brown, light brown and white in color, respectively. The melting points of LIS complexes ranged from 203-

231 ^{o}C (Table 1). These complexes were insoluble in methanol, but partially soluble in both dimethylsulfoxide and dimethylformamide solvents. The suggested formula and morphological structures of the complexes were based on the results of the elemental analyses, molar conductivity, (infrared, UV–visible) spectra, effective magnetic moment in Bohr magnetons, as well as the thermal analysis (TG), and characterized by X-ray powder diffraction (XRD) and scanning electron microscopy (SEM).

Table 1: Analytical and physical data of the LIS complexes

Complexes/ M.Wt. (g/mol)	M.p./(^{o}C)	Λ_m/ ($\Omega^{-1}cm^2 mol^{-1}$)	Elemental analysis/ % found (calcd.)			
			C	H	N	M
LIS 405.488	146-148	14	62.20	7.71	10.36	--
[(Au)$_2$(Cl)$_3$LIS(H$_2$O)].Cl.14H$_2$O 1210.17	203	71	19.62 (20.85)	4.26 (4.92)	3.40 (3.47)	32.38 (32.57)
[PtCl(LIS)NH$_4$.H$_2$O].2Cl.3H$_2$O 795.01	231	121	31.00 (31.73)	4.47 (5.20)	7.00 (7.05)	24.32 (24.54)
[(Zn)$_2$(Cl)$_2$LIS.2H$_2$O].6H$_2$O 749.28	210	33	33.93 (33.66)	5.69 (6.05)	5.52 (5.61)	17.11 (17.45)

The molar conductance values for the Au(III), Pt(IV), and Zn(II) LIS complexes were determined in DMSO at the concentration of (1×10^{-3} mol/cm^3). These values (Table 1) were presence in the range of 33-121 $\Omega^{-1}cm^2mol^{-1}$, but the free ligand has a lower value 14 $\Omega^{-1}cm^2mol^{-1}$. From the results exhibited in Table 1, the Zn(II) complex has non-electrolytic nature, but Au(III) complex has moderated electrolytic behavior. On the other hand, the complex of Pt(IV) has a good electrolyte nature because of its has two ionizable chloride ions in the outer sphere of coordination state [24].

Electronic spectra

Electronic spectra of the lisinopril complexes were recorded in the 200-1000 nm regions in DMSO. There are three detected absorption bands at (225 and 270) and 320 shoulder nm in the electronic spectrum of the free lisinopril ligand, these bands are assigned to π-π* and n-π* transitions, respectively [24]. These transitions occur in case of unsaturated hydrocarbons, which contain carbon atom attached with oxygen atoms as in carboxylic and ketone groups [25]. The bands of the free lisinopril ligand are bathochromically affected (red shifted) clearly in the electronic spectra of the metal complexes indicated the association metal-to-ligand chelations. These results are clearly in accordance with the results of FT-IR and ^{1}H-NMR spectra.
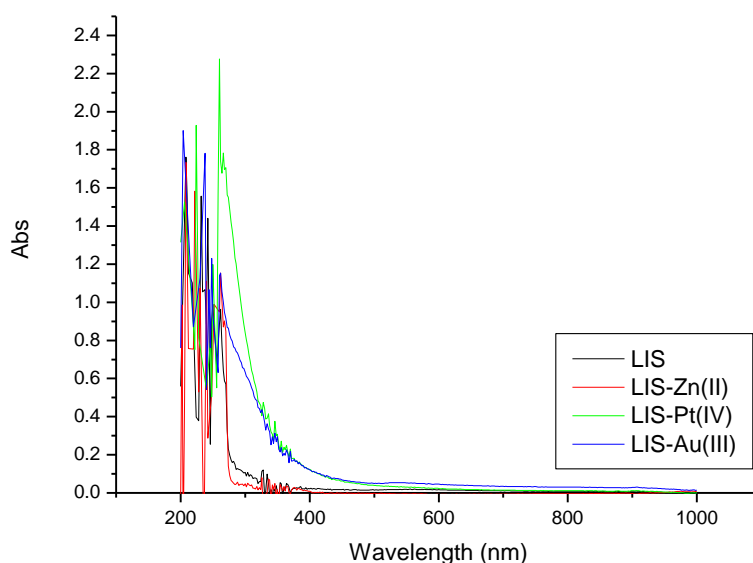
Figure 2: The UV-vis absorption spectra of LIS and their complexes

Infrared spectra

The IR spectra of the LIS complexes were compared with those of the free ligand in order to determine the coordination sites that may be involved in the chelation process. The infrared spectral data of LIS and its complexes are listed in Table 2. There are some guide peaks, in the spectra of the ligand, which are useful in achieving this goal. The position and/or the intensities of these peaks are expected to change upon chelation. In comparison with the published spectra [26-28] of the free LIS spectrum (Figs. 3a), the infrared spectra of LIS complexes (Fig 3b-d) contain the characteristic absorption bands of LIS. The most significant FT-IR bands assignments are listed in (Table 2) and based on the following evidences:

- The infrared spectrum of the free LIS show a sharp band at 3555 cm^{-1}, which is assigned to the v(O–H) stretching vibration of the –OH of carboxylic group. This band became more broadening in case of the spectra of lisinopril complexes due to the presence of the coordinated and uncoordinated water molecules.

- The strong absorption band at 1657 cm^{-1} in the free LIS ligand is assigned to v(C=O) stretching vibration of the carboxylic group [29]. This band has been disappeared in the spectra of LIS metal complexes. This results are supported the deprotonation of COOH group which involvement in the formation of M-O bonds [30, 31]. Another evidence for the participation of the carboxylic group in the coordination is that the band of v(C–O) of carboxylic group in LIS (1233 cm^{-1}) has been red shifted in the metal complexes by Δv= 40-50 cm^{-1}.

- The asymmetric and symmetric stretching vibration motions of carboxylate at 1546 cm^{-1} and 1389 cm^{-1} in the LIS free ligand were shifted toward lower wavenumbers. This indicating that the participation of the carboxylate in the coordination process.

- It is mentioned refer that the coordinative relation between carboxylate and metal ion was mainly dependent on the spectral data between v_{as}(COO$^-$) and v_s(COO$^-$) [32]. The criteria that can be used to distinguish between the three binding states of the carboxylate complexes have been studied previously by Deacon and Phillips [33]. These criteria are: (a) $\Delta v > 200$ cm^{-1} (where Δv =[vas(COO-) - vs(COO-)]) this relation was found in case of monodentate carboxylate complexes, (b) bidentate or chelating carboxylate complexes exhibit Δv significantly smaller than ionic values ($\Delta v < 100$ cm^{-1}), and finally, (c) bridging complexes show Δv comparable to ionic values (Δv ~150 cm^{-1}). Therefore, the difference value Δv is a useful characteristic for determining the coordination mode of the carboxylate group of the ligands. The observed Δv for Au(III), Pt(IV), and Zn(II) complexes (Table 2) located within the range of 91-103 cm^{-1} indicating a bidentate coordination mode for the carboxylate group [34, 35].

- The spectrum of LIS free ligand show absorption bands at 3382 and 3296 cm^{-1} due to v(NH) stretching vibration of –NH and –NH$_2$ groups, respectively. These peaks are slightly down shifted in the complex compared to the same vibration in the pure ligand. This may be refer to the role of the intra- and intermolecular hydrogen bonding, which increased due to the presence of the water molecules after complexation [35].

- An important band of the LIS is that corresponding to v(C=O) stretching vibration of the tertiary amide group, because it is intense and very sensitive to structure features. This sharp peak is changed into broad band upon bonding and slightly shifted to higher wavenumber except for in Zn(II) complex which has an increasing in its intensity because of participation of (C=O) group in formation of intermolecular hydrogen bonding [35].

- The new absorption bands which were observed in the range of (~ 500-600) cm^{-1} are assigned to the stretching absorption band of M-O band [36]. According to the IR data, the LIS coordinated to the metal ions as bidentate ligand via the carboxylate oxygen atoms. Lisinopril has two carboxyl groups including prolyl COOH and central COOH, which can interact with metal ions. In basic medium (pH = 7.4). All carboxylic groups will dissociate to carboxylate ions and own a high electronic density to easily interact with metal ions [27, 37].
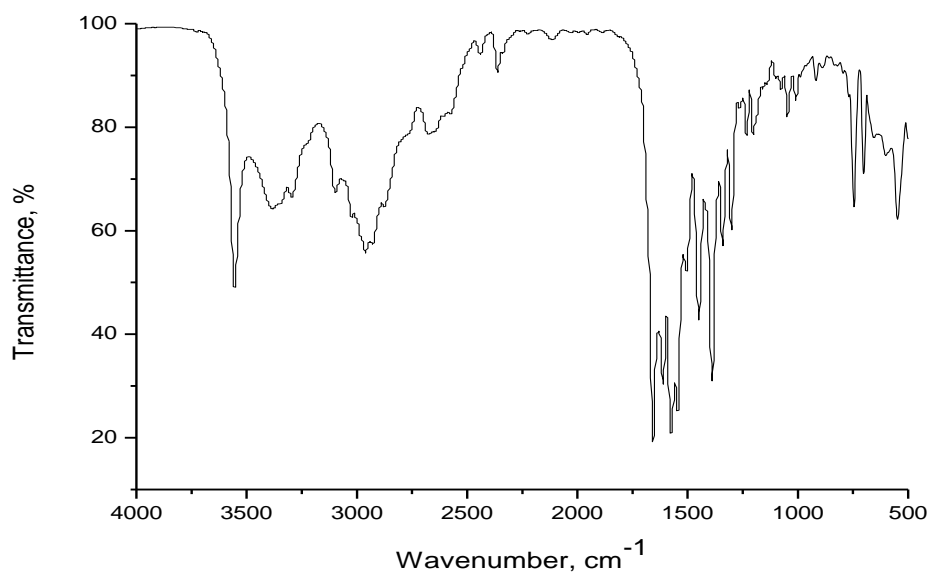
Figure 3a: Infrared spectrum of LIS free ligand
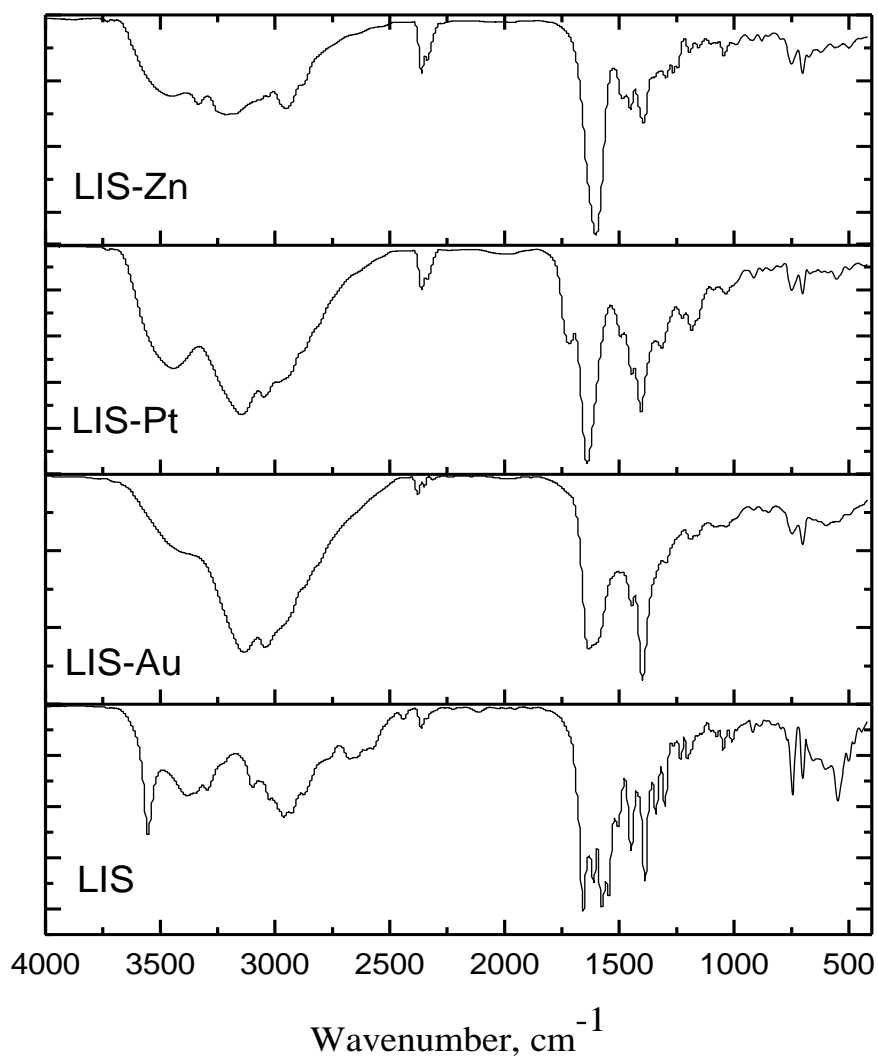
Figure 3b: Infrared spectra of LIS complexes

Table 2: Infrared spectral data of LIS and their complexes

LIS	Au(III)	Pt(IV)	Zn(II)	Assignments
3555	--	3442	3449	$v(OH)$; -OH or H_2O
3383	3133	3145	3333	$v(NH_2)$
3296	3045	3049	3210	$v(NH)$
1657	-	-	-	$v(C=O)$; COOH
1611	1630	1639	1602	$v(C=O)$; amide
1574 1546	1400	1406	1452 <u>1396</u>	$v_{as}(COO^-)$
1389	1298 1189	<u>1315</u> 1226 1185	1396 <u>1298</u>	$v_s(COO^-)$
-	102	<u>91</u>	98	Δv
1233	1189	1226 1185	1194	$v(C–O)$
1449	1447	1447	1452	$v(CH_2)$

^{1}H-NMR spectra
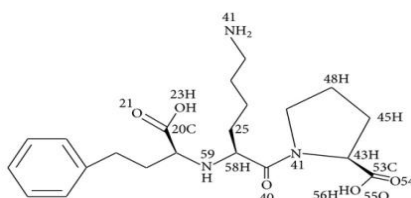
Scheme 1: Proton distributions of LIS drug ligand

Table 3: ^{1}H-NMR spectral data of LIS and their complexes

Compound	δ ppm of hydrogen					
	H; - CH$_2$	H; -NH$_2$	H; -NH-	H; - CH$_2$ pyrollidine	H; -CH aromatic	H; -COOH
LIS	1.55 1.59 1.69 1.70 1.80	2.249 2.500	2.60 2.63 2.72 2.78	3.0-3.6	7.15 7.17 7.20 7.23 7.24 7.27	–
Au(III)	1.55 1.64 1.70 1.80	2.490 2.500	2.60 2.72 2.73 2.80 2.83	3.3-3.6	7.15 7.17 7.20 7.24 7.26 7.29	–
Pt(IV)	1.10 1.20 1.40 1.50 1.79 1.82 1.84 1.85 1.88 1.64	2.49 2.50	2.61 2.69 2.71 2.88	3.0-3.59	7.16 7.18 7.20 7.25 7.27	–
Zn(II)	1.03 1.05 1.08 1.45 1.50 1.85	2.489 2.500	2.66	3.3-3.47	7.19 7.25 7.27	–

^{1}H-NMR chemical shifts of lisinopril free drug has characteristic signals of protons as: δ= 2.00 ppm (s, 1H, NH$_2$), 2.00 ppm (s, 2H, RNH), (1.92 and 2.02) ppm (s, 2H, CH$_2$-pyrollidine), (7.29 and 7.40) ppm (2H, benzyl), 7.27 ppm (s, 1H, benzyl), and 10.5 ppm (s, 1H, COOH). The ^{1}H-NMR spectral data of the LIS free ligand (Scheme 1) show two sets of triplets of unequal intensities. The multiplicity of each signal set reflected first from the interaction of H58 with H25 and H26, giving the two signals in the 3.0–3.6 ppm region, and second from the interaction of H43 with H45 in the 4.1–4.2 ppm region [38]. The ^{1}H-NMR spectra of LIS was compared with its metal complexes. These spectra showed a set of signals which were almost identical to those of parent molecule like, the characteristic peaks of hydrogen for –NH, –NH$_2$, –CH$_2$, and –CH groups of aromatic and pyrollidine ring. This discussion supported that these groups are not involved in the complexation [3, 39].

Thermal analyses and kinetic studies

Thermal analysis of the LIS ligand

The TG curve (Fig. 4) of the lisinopril free ligand shows tow main consecutive steps of mass loss at the temperature ranges (30–800 ^{o}C) with no residue left over at the end of the decomposition process (Table 4). At the first step (30–485 ^{o}C), the mass loss of 51.27 % corresponds to elimination of (5C$_2$H$_2$+CH$_4$+O$_2$+N$_2$)(Cal. = 50.80%). The mass loss (48.73%) at the second step (485–800 ^{o}C) is assigned to a strong releasing the remaining of the LIS molecule with Cal. = 48.83%. The activation energies calculated for the first and second steps are 2.01*10^4 and 1.29*10^5 kJ mol^{-1}, respectively (Table 5). The Δ S*, ΔH* and Δ G* calculated for these steps were (-1.82*10^2 and -1.52*10^2 J k^{-1}mol^{-1}), (1.57*10^4 and 1.21*10^5 kJ mol^{-1}) and (1.12*10^5 and 2.60*10^5 kJ mol^{-1}), respectively. The TGA curves recorded for the Au(III), Pt(II), and Zn(II) lisinopril complexes were given in Fig. 4 and represented in Table 4. These curves, which characterize and compare the thermal decomposition behavior of the ligand and its complexes at the heating rate of 10 ^{o}C min^{-1} under nitrogen, generally show consecutive steps for almost uninterrupted mass losses in the sequential decomposition of these complexes (i.e. no clear plateau between the steps on TG curves) over the experimental temperature range (30–800 ^{o}C).

Thermal analysis of the lisinopril complexes

Table 4 and 5 compare the characteristic thermal and kinetic parameters determined for each step in the decomposition sequence of the complexes. These parameters were determined using Coats–Redfern and Howrtiz Metzger equations [40, 41], and represented as the average values of the two equations. It can be seen clearly that the mass losses (Δm%) obtained from the TGA curves and that calculated for the corresponding molecule, molecules or fragment were in good agreement as was the case for all of these complexes. However, as the compositions of the decomposition products (fragments) of the backbone and of the final decomposition products (i.e. final residues) were not proved, thermal decomposition with ill-defined fragments (i.e. equivalent fragments) and ill-defined final states' products were considered for describing the thermal decomposition of these four complexes. The thermal decomposition process of these four complexes can be described as follows:

Au–LIS

The TG thermogram of [Au$_2$(Cl)$_3$LIS(H$_2$O)].Cl.13H$_2$O (Fig. 4) involves two successive degradation steps at 30–332 and 332–800 ^{o}C. The first step (30 –332 ^{o}C) of 31.48 % mass loss was consistent with the evolution of the uncoordinated water molecules and four molecules of C$_2$H$_2$ (Cal. 30.88%). The second step occurring at 332-800 ^{o}C and it is corresponds to the eliminated of 2C$_2$H$_2$, 4H$_2$O, HNCO, 4H$_2$, N$_2$ and 2Cl$_2$ molecules. At the end of the decomposition process the final residue of an ill-defined state was 41.38% (Cal:.41.44 %), corresponding to gold metal (polluted with few carbon atoms).

Pt– LIS

The thermolysis of [PtCl(LIS)NH$_4$.H$_2$O].2Cl.3H$_2$O (Fig. 4) was characterized by two decomposition steps in the range 30–800 ^{o}C. The first step occurring at (30–259 ^{o}C) and corresponding to the evolution of 4H$_2$O and C$_6$H$_6$ molecules due to weight loss of 19.61% and its calculated value is 18.82%. The second step occurring at (259-800 ^{o}C) is corresponding to the loss of 2C$_6$H$_6$, C$_2$H$_2$, HCl, Cl$_2$, 2N$_2$, CO, 4H$_2$O and 2H$_2$ molecules, representing a weight loss of 57.08% and its calculated value is 56.39%. At the end of the decomposition

process, the total residual mass of 23.32% is in agreement with the final product of platinum metal (Cal. 24.47%).

Zn– LIS

The thermolysis of $[(Zn)_2(Cl)_2LIS.2H_2O].6H_2O$ as it follows from (Fig. 4) and referred in Table 4 reveals three decomposition steps at 30–237, 237–295 and 295-800 °C. The first mass loss occurred between 30 and 237 °C is due to dehydration of eight water molecules, with a loss of 18.32% which is closed matching with theoretical calculation 19.22%. The second stage, from 237-295 °C is due to the initial decomposition of this complex, the mass loss of 16.75% was consistent with the release of $4C_2H_2$, $\frac{1}{2}H_2$ and $\frac{1}{2}O_2$ molecules, with Cal. 15.88%. The third-step (295-800) was assigned to the elimination of $2C_6H_6$, H_2O, N_2, $3H_2$, Cl_2 and O_2 molecules, representing a weight loss of 41.88% and its calculated value is 41.50%. At the end of the decomposition presses, the total residual mass of 23.22% is in agreement with the final product of zinc oxide polluted with few carbon atoms (Cal. 23.33%).

Table 4: Thermogravimetric data of LIS and their complexes

Compounds	Steps	Temp /(°C)	Decomposed assignments	Weight loss Found (calcd; %)
LIS drug	1st	25-485	$-5C_2H_2 +CH_4 +O_2 + N_2$	51.27(50.80)
	2nd	485-800	$-5C_2H_2 +2H_2O+NO+H_2$	48.73(48.83)
	Residue (nil)			--
$[Au_2(Cl)_3LIS(H_2O)].Cl.14H_2O$	1st	30-332	$-4C_2H_2+15H_2O$	31.48(30.88)
	2nd	332-800	$-2C_2H_2+4H_2O+HNCO+4H_2+N_2+2Cl_2$	27.06(27.31)
	Residue (2Au(0) metal + few carbons)			41.38(41.44)
$[PtCl(LIS)NH_4.H_2O].2Cl.3H_2O$	1st	30-259	$- C_6H_6+4H_2O$	19.61(18.82)
	2nd	259-800	$-2C_6H_6+C_2H_2+HCl+Cl_2+2N_2+CO+ 4H_2O+2H_2$	57.08(56.39)
	Residue Pt(0) metal			23.32(24.47)
$[(Zn)_2(Cl)_2 LIS. 2H_2O].6H_2O$	1st	30-237	$-8H_2O$	18.32(19.22)
	2nd	237-295	$- 4C_2H_2+\frac{1}{2}H_2+\frac{1}{2}O_2$	16.75(15.88)
	3rd	295-800	$-2C_6H_6+H_2O +N_2 +3H_2+ Cl_{2+}O_2$	41.88(41.50)
	Residue (2 ZnO+ few carbons)			23.22(23.33)
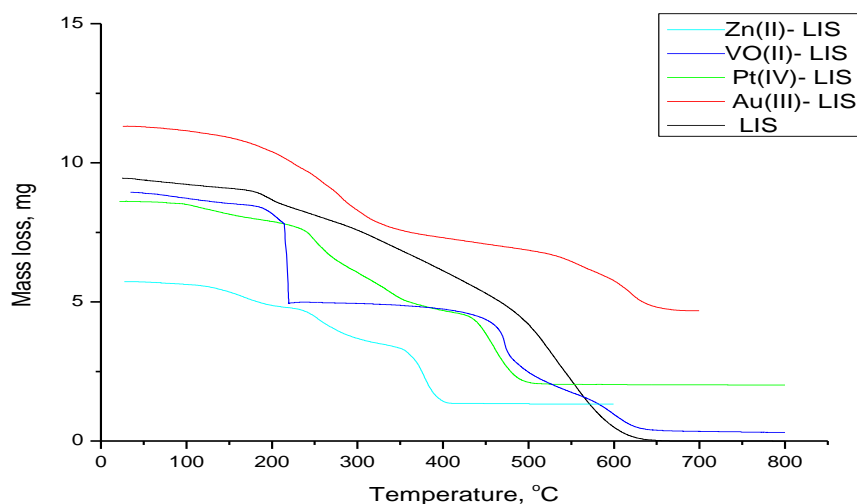
Figure 4: TG curves of LIS free ligand and their complexes

The different thermodynamic parameters of the complexes were listed in Table 5. The activation energies of decomposition found to be in the range 2.82×10^4-1.59×10^5 kJmol^{-1}. The high values of the activation energies reflect the thermal stability of the complexes. The entropy of activation found to have negative values in all the complexes, which indicate that the decomposition reactions proceed with a lower

rate than the normal ones. On another meaning the thermal decomposition process of all LIS complexes are non-spontaneous, i.e, the complexes are thermally stable. The correlation coefficients of the Arhenius plots of the thermal decomposition steps found to lie in the range 0.9529 to 0.9964, showing a good fit with linear function.

Table 5: Kinetic thermodynamic data of LIS and their complexes

Compound	stages	Method	Parameter					
			E (kJ mol^{-1})	A (s−1)	ΔS^* (J k^{-1}mol^{-1})	ΔH^* (kJ mol^{-1})	ΔG^* (kJ mol^{-1})	r
LIS	1st	CR	$1.52*10^4$	$1.22*10^7$	$-1.14*10^2$	$1.08*10^4$	$7.10*10^4$	0.9888
		HM	$2.51*10^4$	$8.22*10^{-1}$	$-2.51*10^2$	$2.07*10^4$	$1.53*10^5$	0.9953
		average	$2.01*10^4$	$6.10*10^6$	$-1.82*10^2$	$1.57*10^4$	$1.12*10^5$	0.9920
	2nd	CR	$1.15*10^5$	$6.76*10^4$	$-1.62*10^2$	$1.07*10^5$	$2.55*10^5$	0.9974
		HM	$1.43*10^5$	$7.33*10^5$	$-1.42*10^2$	$1.35*10^5$	$2.65*10^5$	0.9947
		average	$1.29*10^5$	$4.00*10^5$	$-1.52*10^2$	$1.21*10^5$	$2.60*10^5$	0.9960
Au-LIS	1st	CR	$2.37*10^4$	$1.16*10^6$	$-1.32*10^2$	$1.99*10^4$	$8*10^4$	0.9963
		HM	$3.28*10^4$	$2.81*10$	$-2.21*10^2$	$2.90*10^4$	$1.90*10^5$	0.9979
		average	$2.82*10^4$	$5.80*10^5$	$-1.76*10^2$	$2.44*10^4$	$1.35*10^5$	0.9971
	2nd	CR	$5.35*10^4$	$4.56*10^5$	$-1.45*10^2$	$4.65*10^4$	$1.68*10^5$	0.9435
		HM	$7.42*10^4$	$1.31*10^2$	$-2.13*10^2$	$6.72*10^4$	$2.46*10^5$	0.9821
		average	$6.38*10^4$	$2.28*10^5$	$-1.79*10^2$	$5.68*10^4$	$2.07*10^5$	0.9628
Pt-LIS	1st	CR	$3.03*10^4$	$1.10*10^5$	$-1.51*10^2$	$2.68*10^4$	$8.99*10^4$	0.9862
		HM	$4.07*10^4$	$8.77*10^2$	$-1.91*10^2$	$3.73*10^4$	$1.17*10^5$	0.9790
		average	$3.55*10^4$	$5.5438*10^4$	$-1.71*10^2$	$3.20*10^4$	$1.03*10^5$	0.9826
	2nd	CR	$3.30*10^4$	$1.58*10^6$	$-1.35*10^2$	$2.63*10^4$	$1.34*10^5$	0.9431
		HM	$5.06*10^4$	$4.64*10^{10}$	$-2.40*10^2$	$4.40*10^4$	$2.37*10^5$	0.9627
		average	$4.18*10^4$	$2.32*10^{10}$	$-1.87*10^2$	$3.51*10^4$	$1.85*10^5$	0.9529
Zn-LIS	1st	CR	$5.08*10^4$	$5.43*10^4$	$-1.57*10^2$	$2.75*10^4$	$9.13*10^4$	0.994
		HM	$3.87*10^4$	$6.53*10^2$	$-1.94*10^2$	$3.53*10^4$	$1.14*10^5$	0.9989
		average	$4.47*10^4$	$2.75*10^4$	$-1.75*10^2$	$3.14*10^4$	$1.03*10^5$	0.9964
	2nd	CR	$1.54*10^5$	$1.01*10^{13}$	$-9.03*10^{-1}$	$1.50*10^5$	$1.50*10^5$	0.9786
		HM	$1.64*10^5$	$1.21*10^{14}$	$1.98*10$	$1.59*10^5$	$1.49*10^5$	0.9768
		average	$1.59*10^5$	$6.55*10^{13}$	18.90	$1.54*10^5$	$1.49*10^5$	0.9777
	3nd	CR	$7.09*10^4$	$2.59*10^3$	$-1.87*10^2$	$6.49*10^4$	$2.00*10^5$	0.8767
		HM	$8.64*10^4$	$9.25*10^3$	$-1.76*10^2$	$8.04*10^4$	$2.07*10^5$	0.8788
		average	$7.86*10^4$	$5.92*10^3$	$-1.81*10^2$	$7.26*10^4$	$2.03*10^5$	0.8777

SEM and XRD studies

The morphological surfaces of Zn(II), Au(III) and Pt(IV) with LIS complexes were checked upon scanning electron microscopy technique. Scanning electron micrographs are shown in Fig 5A-D. The surface morphology of SEM micrograph reveals the well sintered nature of the complexes with variant grain sizes and shapes. The distribution of the grain size is homogeneous except for Pt-LIS complex (Fig. 5C), where small-to-medium particles of nearly same size. Clear regular distribution grains are obtained with agglomerates for Zn(II) complex (5B). The particle size distribution of the LIS complexes was evaluated and the average particle sizes of these were found to be 10-500 µm range. The X-ray powder diffraction patterns in the range of 4°< 2θ < 80° for the Zn(II), Au(III) and Pt(IV)-LIS complexes were carried in order to obtain an idea about the lattice dynamics of the resulted complexes. X-ray diffraction of these complexes were recorded and shown in Fig. 6A-D. The values of 2θ, d value (the volume average of the crystal dimension normal to diffracting plane), full width at half maximum (FWHM) of prominent intensity peak, relative intensity (%) and particle size of complexes were calculated. The XRD features of Zn(II) and Pt(IV)-LIS complexes are amorphous shape except for gold(II)-LIS is crystalline structure with maximum diffraction pattern at 2θ/d-value(Ǻ)= 38/1220. The crystallite size could be estimated from XRD patterns by applying FWHM of the characteristic peaks using Deby-Scherrer equation 1 [42].

$$D= K\lambda/\beta Cos\theta \ldots\ldots.. (equ. 1)$$

Where D is the particle size of the crystal gain, K is a constant (0.94 for Cu grid), λ is the x-ray wavelength (1.5406 Å), θ is the Bragg diffraction angle and β is the integral peak width. The particle size was estimated according to the highest value of intensity compared with the other peaks. The data of gold(III)-LIS complex gave an impression that the particle size located within nano scale range.
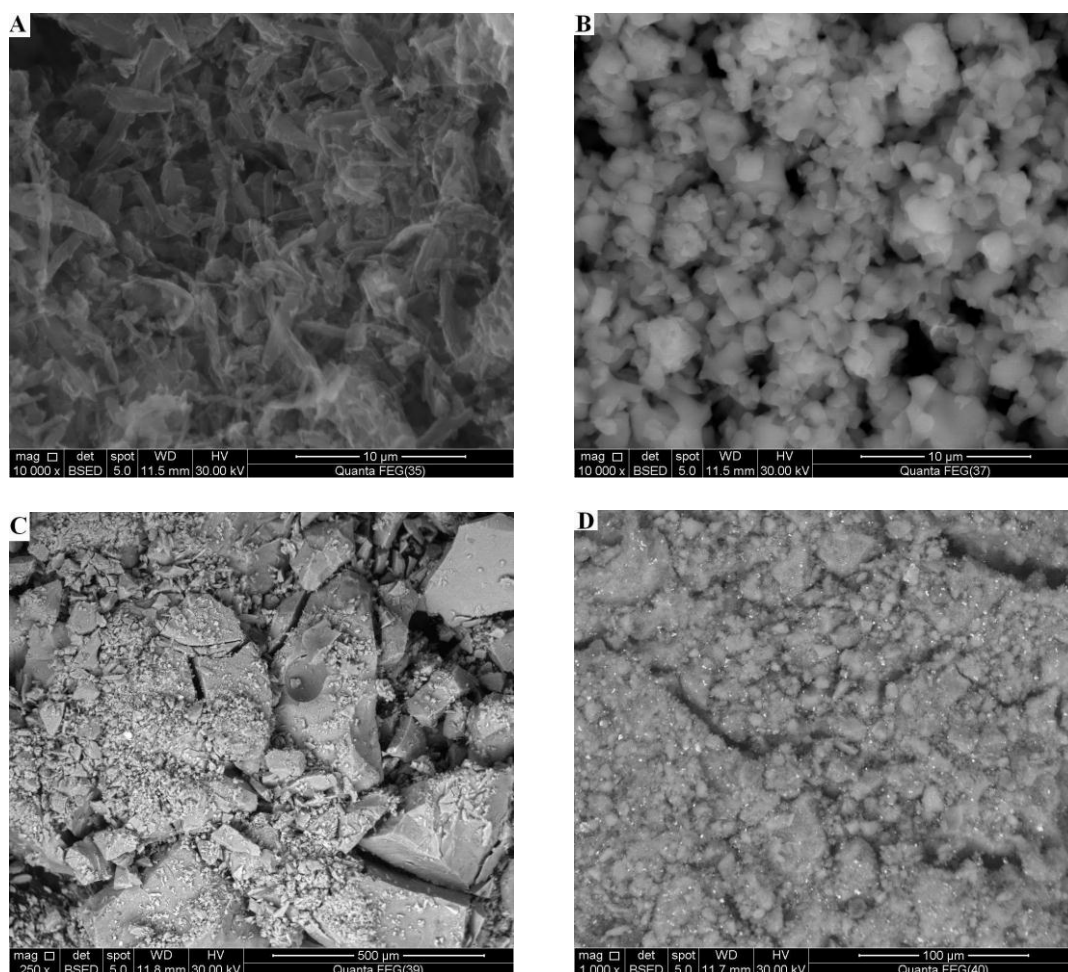
Figure 5: SEM images of A-LIS, B-Zn(II)-LIS, C-Pt(IV)-LIS, and D-Au(III)-LIS complexes

The structures of the complexes of LIS with Zn(II), Au(III) and Pt(IV) ions have been confirmed form the elemental analyses, IR, ^{1}H-NMR, molar conductance, UV-Vis, and thermal analysis data. Thus, from the IR spectra, it is concluded that LIS behaves as a mono- or di- basic bidentate ligand coordinated to the metal ions via the deprotonated –OH of COOH group. From the molar conductance data, it is found that the complexes are electrolytes except for Zn(II) complexes. Because of the above observations, the coordinated geometries are suggested for the investigated complexes. As a general conclusion, the investigated complexes structures can be given as shown in Figs. 7.

Antimicrobial studies

The antimicrobial test in *vitro* of the LIS ligand and their metal complexes clearly show that the compounds have both antibacterial and antifungal potency against the tested organisms. The complexes showed more activity than free ligand. Biological studies were observed in term antimicrobial activities of target complexes against gram-positive (*Staphylococcus aureus*) and gram-negative (*Escherichia coli*) and two strains of fungus (*Aspergillus flavus* and *Candida albicans*). Result from the agar disc diffusion tests for antimicrobial activities of target compounds are presented in Table 6. By comparison between the biological evaluation of LIS complexes with the standards Tetracycline as (antibacterial agent) and Amphotericin B as (antifungal agent), the results of highest-to-lowest effective can be summarized as follows;

i-   *Escherichia coli*   Au(III)> Zn(II)>Pt(IV)
ii- *Staphylococcus aureus*   Zn(II)>Au(III)>Pt(IV)
iii- *Aspergillus flavus*   Au(III)>Pt(IV)>Zn(II)
iv- *Candida albicans*   Pt(IV)>Au(III)>Zn(II)

possible mode for increase in antibacterial activity may be considered in light of overtone's concept [43] and Tweedy's chelation theory [44]. On chelation, the polarity of the metal ion will be reduced to a greater extent due to the overlap of the ligand orbital and partial sharing of the positive charge of the metal ion with donor groups [45]. The interaction between metal ion and the lipid is favored. This may lead to the breakdown of the permeability barrier of the cell, resulting in interference with normal cell processes.
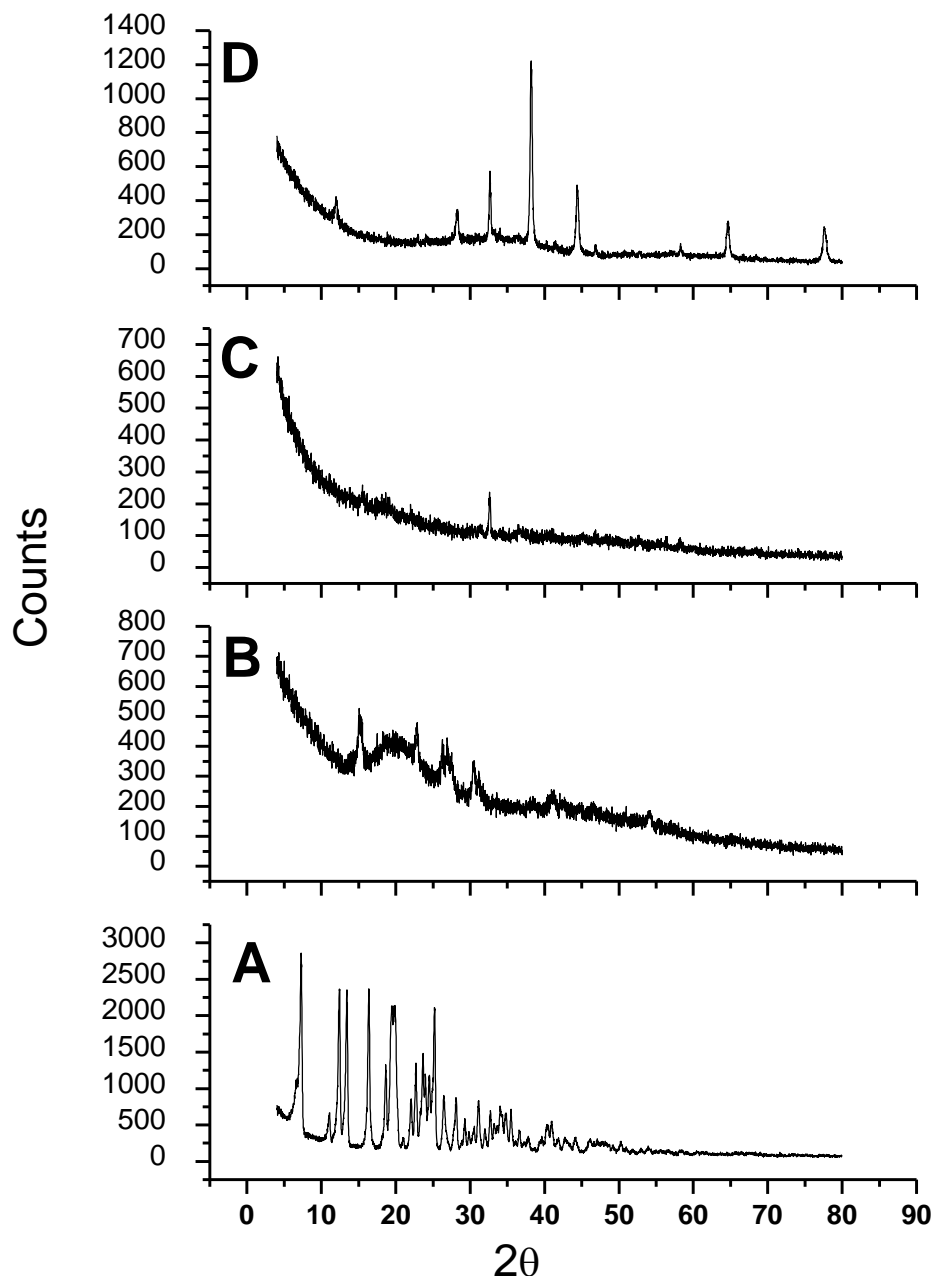
Figure 6: XRD spectra of A-LIS, B-Zn(II)-LIS, C-Pt(IV)-LIS, and D-Au(III)-LIS complexes
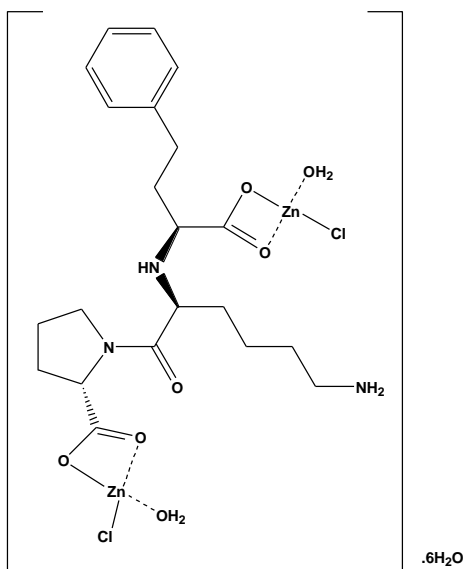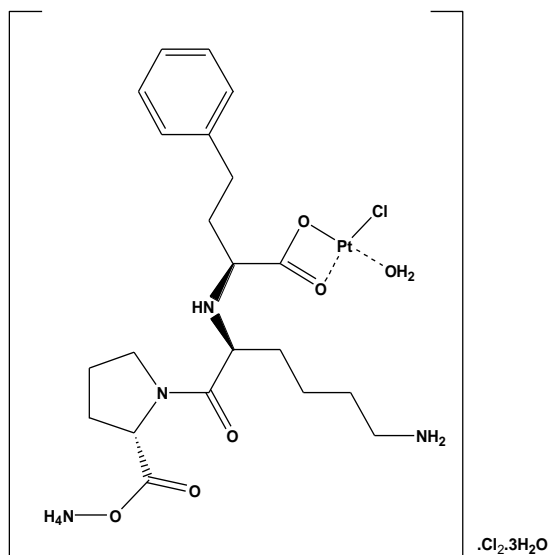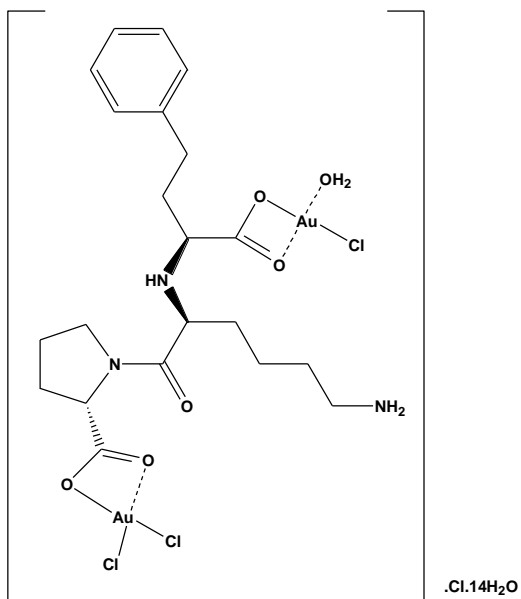
Figure 7: Suggested structures of Zn(II), Au(III) and Pt(IV)-LIS complexes

Table 6: The inhibition zone diameter (mm/mg sample) of LIS complexes against some kind of bacteria and fungi

Sample		Inhibition zone diameter (mm / mg sample)			
		Escherichia coli (G⁻)	*Staphylococcus aureus* (G⁺)	*Aspergillus flavus* (Fungus)	*Candida albicans* (Fungus)
Control: DMSO		0.0	0.0	0.0	0.0
Standard	Tetracycline Antibacterial agent	32	30	--	--
	Amphotericin B Antifungal agent	--	--	18	19
Lis		0.0	0.0	0.0	0.0
Zn(II)		8	14	3.0	1.0
Au(III)		14	7.0	9.0	4.0
Pt(IV)		6.0	4.0	8.0	6.0

REFERENCES

[1] S.R. Pattan, S.B. Pawar, S.S. Vetal, U.D. Gharate, S.B. Bhawar, Indian Drugs, 49(11), November (2012).
[2] M.S. Refat, S.F. Mohamed, Spectrochimica Acta A, 82 (2011) 108.
[3] M.S. Refat, J. Mol. Str., 969 (2010) 163.
[4] M.S. Refat, S.A. El-Shazly, Eur. J. Med. Chem., 45(7) (2010) 3070.
[5] J.G. Cleland, Int. J. Clin. Pract.,108 (1999) 7.
[6] M. Burnier, H.R. Brunner, Lancet, 355 (2000) 637.
[7] The Merck Index. 13th ed., Merck Research Lab publishers, White House Station, NJ, US, 2001.
[8] J. Wong, R.A. Patel, P.R. Kowey, Progress in Cardiovascular Diseases, 47 (2004) 116.
[9] B. Beermann, American Journal of Medicine, 85(3B) (1988) 25.
[10] Indian Pharmacopoeia. Ministry of Health and Family Welfare New Delhi, 2007, 2, pp. 1306-08
[11] British Pharmacopoeia. Stationery Office Books (TSO) London, United Kingdom, 2005, 2, pp. 1199.
[12] United States Pharmacopoiea-USP-24, NF-19, Asian Edition, United States Pharmacopoeial Convention, INC. Twin brook Parkway, Rockville, MD, U.S.A. 2000, pp. 979.
[13] N. Rahman, N. Anwar, M. Kashif, Il Farmaco, 60 (2005) 605.
[14] C.A. Beasley, J. Shaw, Z. Zhao, R.A. Reed, Journal of Pharmaceutical and Biomedical Analysis, 37 (2005) 559.
[15] A. El-Gindy, A. Ashour, L. Abdel-Fattah, M.M. Shabana, Journal of Pharmaceutical and Biomedical Analysis, 25 (2001) 923.
[16] S. Hillaert, W. Van den Bossche, Journal of Pharmaceutical and Biomedical Analysis, 25 (2001) 775-783.
[17] A.S. Yuan, J.D. Gilbert, J. Pharm. Biomed. Anal., 14(7) (1996) 773.
[18] K. Shepley, M.L. Rocci, H. Patrick, J. Pharm. Biomed. Anal. 6(3) (1988) 241.
[19] L. Abdel-Fattah, A. El-Kosasy, L. Abdel-Aziz, J. Am. Sci., 6(10) (2010) 1115.
[20] W. Shun-Li, C. Chi-Hsiang, L. Shan-Yang, Chem. Pharm. Bull., 50(1) (2002) 78.
[21] J.A. Balman, G.L. Christie, J.R. Duffield, D.R. Williams, Inorganica Chimica Acta, I52 (1988) 81-90
[22] M. Zaky, M.Y. El-Sayed1, S.M. El-Megharbel, S. Abo Taleb, M.S. Refat, J. Mex. Chem. Soc., 58(2) (2014) 142.
[23] A.W. Bauer, W.M. Kirby, C. Sherris, M. Turck, Amer. J. Clinical Pathology, 45 (1966) 493.
[24] M.S. Refat, Spectrochim. Acta Part A, 68 (2007) 1393.
[25] S. Dinç, Ö.A. Dönmez, B. Asçi, A.E. Bozdogan, Asian Journal of Chemistry, 25(2) (2013) 999.
[26] A. Olaru, Gh. Borodi, I. Kacsó, M. Vasilescu, I. Bratub, O. Cozar, Spectroscopy, 23 (2009) 191.
[27] S.-L. Wang, C.-H. Chuang, S.-Y. Lin, Chem. Pharm. Bull., 50(1) (2002) 78.
[28] S.-L. Wang, S.-Y. Lin, T.-F. Chen, Chem. Pharm. Bull. 48(12) (2000) 1890.
[29] S.A. Sadeek, A.M. El-Didamony, W.H. El-Shwiniy, W.A. Zordok, J. Arg. Chem. Soc., 97 (2009) 51.
[30] A.A. Adam, J. Mat. Sci. Res., 1 (2012) 167.
[31] M.S. Refat, Spectrochimica Acta Part A 105 (2013) 326.
[32] S.D. Robinson, M.F. Uttley, J. Chem. Soc., Dalton, 1973, 1912.
[33] G.B. Deacon, R.J. Phillips, Coord. Chem. Rev., 33 (1980) 227.

[34] C. Dendrinou-Samara, G. Tsotsou, L.V. Ekateriniadou, A.H. Kortsaris, C.P. Raptopoulou, A. Terzis, D.A. Kyriakidis, D.P. Kessissoglou, J. Inorg. Biochem., 71 (1998) 171.

[35] K. Nakamoto, Infrared and Ramman Spectra of Inorganic and Coordination Compounds, (4th ed.), New York: Wiley. pp. 230,

[36] 1986.

[37] S. Sharma, S.A. Iqbal, M. Bhattacharya, Orient. J. Chem., 25(4) (2009) 1101.

[38] S. Bouabdallah, Med Thaie, Ben Dhia, Med Rida Driss1, International Journal of Analytical Chemistry, Volume 2014, Article ID 494719, 8 pages.

[39] M.S. Arayne, N. Sultana, A. Tabassum, Open Journal of Biochemistry, 1(2) (2014) 2374.

[40] H.H. Horowitz, G. Metzger, Anal. Chem. 35 (1963) 1464.

[41] W. Coats, J. P. Redfern, Nature (London) 201 (1964) 68.

[42] C.X. Quan, L.H. Bin, G.G. Bang, Mater. Chem. Phys. 91 (2005) 317.

[43] M.N. Patel, P.B. Pansuriya, P.A. Parmar, D.S. Gandhi1, Pharma. Chem., J., 42(12) (2008) 687.

[44] B.G. Tweedy, Phytopathology, 55 (1964) 910.

[45] P.K. Panchal, P.B. Pansuriya, M.N. Patel, J. Enz. Inhib. Med. Chem., 21 (2006) 203.